Langmuir
Article
pubs.acs.org/Langmuir

Self-Assembled Nanogel Made of Mannan: Synthesis and Characterization

Sílvia A. Ferreira,[†] Paulo J. G. Coutinho,[‡] and Francisco M. Gama*,[†]

[†]*IBB-Institute for Biotechnology and Bioengineering, Centre for Biological Engineering, University of Minho, Campus Gualtar, 4710-057 Braga, Portugal, and* [‡]*Centre of Physics, University of Minho, Campus Gualtar, 4710-057 Braga, Portugal*

Received March 4, 2010. Revised Manuscript Received May 16, 2010

Amphiphilic mannan (mannan-C_{16}) was synthesized by the Michael addition of hydrophobic 1-hexadecanethiol (C_{16}) to hydroxyethyl methacrylated mannan (mannan-HEMA). Mannan-C_{16} formed nanosized aggregates in water by self-assembly via the hydrophobic interaction among C_{16} molecules as confirmed by hydrogen nuclear magnetic resonance (^{1}H NMR), fluorescence spectroscopy, cryo-field emission scanning electron microscopy (cryo-FESEM), and dynamic light scattering (DLS). The mannan-C_{16} critical aggregation concentration (cac), calculated by fluorescence spectroscopy with Nile red and pyrene, ranged between 0.04 and 0.02 mg/mL depending on the polymer degree of substitution of C_{16} relative to methacrylated groups. Cryo-FESEM micrographs revealed that mannan-C_{16} formed irregular spherical macromolecular micelles, in this work designated as nanogels, with diameters ranging between 100 and 500 nm. The influence of the polymer degree of substitution, DS_{HEMA} and $DS_{C_{16}}$, on the nanogel size and zeta potential was studied by DLS at different pH values and ionic strength and as a function of mannan-C_{16} and urea concentrations. Under all tested conditions, the nanogel was negatively charged with a zeta potential close to zero. Mannan-C_{16} with higher DS_{HEMA} and $DS_{C_{16}}$ values formed larger nanogels and were also less stable over a 6 month storage period and at concentrations close to the cac. When exposed to solutions of different pH and aggressive conditions of ionic strength and urea concentration, the size of mannan-C_{16} varied to some extent but was always in the nanoscale range.

Introduction

The self-assembly phenomenon has been defined as the autonomous, spontaneous, and reversible organization of molecular units into structurally stable and well-defined aggregates in which defects are energetically rejected. This process is cost-effective, versatile, and facile.[1−3] Self-assembly occurs toward the system's thermodynamic minima and through a balance of attractive and repulsive interactions, which are generally weak and noncovalent, such as electrostatic, van der Waals, and Coulomb interactions, hydrophobic forces, and hydrogen bonds.[4]

Above the critical aggregation concentration (cac), amphiphilic polymers can self-assemble in water because of hydration forces, namely, intra- and/or intermolecular hydrophilic and hydrophobic interactions.[5] In other words, the nanostructure builds itself.

Recently, different hydrophobically modified polymers have been designed as new solutions for multifunctional pharmaceutical nanocarriers. A variety of molecules can be encapsulated within the particle core, entrapped in the polymer matrix, chemically attached, and/or physically adsorbed at the surface of the macromolecular micelles, also designated by some authors as nanogels. In this work, we adopt this terminology, with the term nanogel referring to the hydrogel-like—highly porous and hydrated—nanosized material. Through combining several useful properties in one nanogel, the possibility to enhance the efficacy of many therapeutic and diagnostic protocols arose.[6]

Various macromolecular polysaccharides have been reported as molecular carriers, including chitosan,[7] dextran,[8] dextrin,[9] mannan,[10,11] pullulan,[10,12,13] hyaluronic acid,[14] either in their native forms or as carrier conjugates.[15] Among them, we selected mannan, from *Saccharomyces cerevisiae*, which consists of an α-1,6-linked mannose backbone with a high percentage of α-1,2 and α-1,3 side chains of different composition.[16] Mannan is a biodegradable, biocompatible polymer and has been described as a promising targeted delivery system.[10,17−19] Mannan potentially targets antigen-presenting cells (APCs) because dendritic cells and macrophages express on their surface mannose receptor, which recognizes carbohydrates present on the cell walls of infectious agents. The mannose receptor is part of the multilectin receptor proteins and provides a link between innate and adaptive immunity.[19−22]

*Corresponding author. E-mail: fmgama@deb.uminho.pt.

(1) Whitesides, G. M.; Mathias, J. P.; Seto, C. T. *Science* **1991**, *254*, 1312–1319.
(2) Whitesides, G. M.; Grzybowski, B. *Science* **2002**, *295*, 2418–2421.
(3) Halley, J. D.; Winkler, D. A. *Complexity* **2008**, *14*, 10–17.
(4) Whitesides, G. M.; Boncheva, M. *Proc. Natl. Acad. Sci. U.S.A.* **2002**, *99*, 4769–4774.
(5) Huie, J. C. *Smart Mater. Struct.* **2003**, *12*, 264–271.
(6) Torchilin, V. P. *Adv. Drug Delivery Rev.* **2006**, *58*, 1532–1555.
(7) Park, J. H.; Kwon, S. G.; Nam, J. O.; Park, R. W.; Chung, H.; Seo, S. B.; Kim, I. S.; Kwon, I. C.; Jeong, S. Y. *J. Controlled Release* **2004**, *95*, 579–588.
(8) Hennink, W. E.; Talsma, H.; Borchert, J. C. H.; DeSmedt, S. C.; Demeester, J. *J. Controlled Release* **1996**, *39*, 47–55.
(9) Goncalves, C.; Martins, J. A.; Gama, F. M. *Biomacromolecules* **2007**, *8*, 392–398.
(10) Gu, X. G.; Schmitt, M.; Hiasa, A.; Nagata, Y.; Ikeda, H.; Sasaki, Y.; Akiyoshi, K.; Sunamoto, J.; Nakamura, H.; Kuribayashi, K.; Shiku, H. *Cancer Res.* **1998**, *58*, 3385–3390.
(11) Tang, C. K.; Lodding, J.; Minigo, G.; Pouniotis, D. S.; Plebanski, M.; Scholzen, A.; McKenzie, I. F.; Pietersz, G. A.; Apostolopoulos, V. *Immunology* **2007**, *120*, 325–335.
(12) Akiyoshi, K.; Kobayashi, S.; Shichibe, S.; Mix, D.; Baudys, M.; Kim, S. W.; Sunamoto, J. *J. Controlled Release* **1998**, *54*, 313–320.
(13) Na, K.; Bae, Y. H. *Pharm. Res.* **2002**, *19*, 681–688.
(14) Choi, K. Y.; Min, K. H.; Na, J. H.; Choi, K.; Kim, K.; Park, J. H.; Kwon, I. C.; Jeong, S. Y. *J. Mater. Chem.* **2009**, *19*, 4102–4107.
(15) Coviello, T.; Matricardi, P.; Marianecci, C.; Alhaique, F. *J. Controlled Release* **2007**, *119*, 5–24.
(16) Nakajima, T.; Ballou, C. E. *J. Biol. Chem.* **1974**, *249*, 7685–7694.
(17) Apostolopoulos, V.; Pietersz, G. A.; Loveland, B. E.; Sandrin, M. S.; McKenzie, I. F. *Proc. Natl. Acad. Sci. U.S.A.* **1995**, *92*, 10128–10132.
(18) Sihorkar, V.; Vyas, S. P. *J. Pharm. Pharm. Sci.* **2001**, *4*, 138–158.
(19) Gupta, A.; Gupta, R. K.; Gupta, G. S. *J. Sci. Ind. Res.* **2009**, *68*, 465–483.
(20) Avrameas, A.; McIlroy, D.; Hosmalin, A.; Autran, B.; Debre, P.; Monsigny, M.; Roche, A. C.; Midoux, P. *Eur. J. Immunol.* **1996**, *26*, 394–400.
(21) Fukasawa, M.; Shimizu, Y.; Shikata, K.; Nakata, M.; Sakakibara, R.; Yamamoto, N.; Hatanaka, M.; Mizuochi, T. *FEBS Lett.* **1998**, *441*, 353–356.
(22) Apostolopoulos, V.; McKenzie, I. F. *Curr. Mol. Med.* **2001**, *1*, 469–474.

In this study, we aimed to develop new amphiphilic conjugates by the Michael addition of hydrophobic 1-hexadecanethiol (C_{16}) to hydroxyethyl methacrylated mannan (mannan-HEMA), also produced in this work. We studied the self-assembly of mannan-C_{16} in an aqueous environment by ^{1}H NMR and fluorescence spectroscopy with hydrophobic fluorescent probes Nile red and pyrene. Relevant features such as the chemical structure, size, surface charge, and morphology of the mannan-C_{16} nanogel were characterized using ^{1}H NMR spectroscopy, cryo-field emission scanning electron microscopy (cryo-FESEM), and dynamic light scattering (DLS).

Materials and Methods

Materials. CDI-activated hydroxyethyl methacrylate (HEMA-CI) was produced as described by van Dijk-Wolthuis et al.[23] Mannan (from *S. cerevisiae*), dimethyl sulfoxide (DMSO), 4-(*N*,*N*-dimethylamino)pyridine (DMAP), triethylamine (TEA), 1-hexadecanethiol, deuterium oxide (D_2O), dimethyl sulfoxide-d_6 (DMSO-d_6), pyrene (Py), and 9-(diethylamino)-5H-benzo[α]phenoxazin-5-one (Nile red, NR) were purchased from Sigma-Aldrich. Pyrene was purified by appropriate recrystallization from absolute ethanol. Phosphotungstic acid was purchased from Riedel-de Haën. Regenerated cellulose tubular membranes, with a 12 000−14 000 nominal MWCO, were obtained from Membrane Filtration Products. Water was purified with a Milli-Q system (Millipore). Other organic and inorganic chemicals were purchased from Sigma-Aldrich and used without further purification.

Synthesis of Amphiphilic Mannan-C_{16}. HEMA-derivatized mannan (mannan-HEMA) was prepared as described by van Dijk-Wolthuis et al.[23] Briefly, mannan was dissolved in dry DMSO in a nitrogen atmosphere to a concentration of 3−5% w/v with different calculated amounts of HEMA-CI resulting in 0.25 and 0.4 molar ratios of HEMA-CI to mannose residues. The reaction catalyzed by DMAP (2 mol equiv to HEMA-CI) was allowed to proceed, and the mixture was stirred at room temperature for 4 days. The reaction was terminated with concentrated HCl (2% v/v), which neutralized DMAP and imidazole. The mixture was then dialyzed against frequently changed distilled water at 4 °C for 3 days. After being lyophilized, mannan-HEMA resulted as a pallid-yellow, fluffy product that was stored at −20 °C. Finally, amphiphilic molecule mannan-HEMA-SC_{16} (mannan-C_{16}) was produced as described elsewhere.[9] Briefly, mannan-HEMA and C_{16} at 1, 1.2, and 2 molar ratios of C_{16} to HEMA-CI were mixed in DMSO (equivalent HEMA = 0.03 M). The reaction mixture catalyzed by TEA (2 mol equiv with respect to HEMA) was stirred for 3.5 days at 50 °C. The resulting mixture was dialyzed for 3 days against frequently changed distilled water at room temperature. After being lyophilized, mannan-C_{16} resulted as a pallid-yellow, fluffy product that was stored at −20 °C.

^{1}H NMR Spectroscopy. Lyophilized reaction products were dispersed in D_2O (5 mg/mL). Mannan-C_{16} was also dispersed in DMSO-d_6 and in 10% D_2O-DMSO-d_6 (5 mg/mL). Samples were stirred overnight at 50 °C to obtain a clear dispersion, which was transferred to 5 mm NMR tubes. One-dimensional ^{1}H NMR measurements were performed with a Varian Unity Plus 300 spectrometer operating at 299.94 MHz. One-dimensional ^{1}H NMR spectra were recorded at 298 K with 256 scans, a spectral width of 5000 Hz, a relaxation delay of 1 s between scans, and an acquisition time of 2.8 s.

Fluorescence Spectroscopy. The cac of mannan-C_{16} was fluorometrically investigated using hydrophobic guest molecules such as NR and Py, whose maximum solubility values in water are 1×10^{-6} and 5×10^{-7} M, respectively. The fluorescence intensity change of these guest molecules was calculated as a function of the mannan-C_{16} concentration. Lyophilized mannan-C_{16} was dispersed in ultrapure water (1 mg/mL) with stirring for 3 days at 50 °C. Consecutive dilutions of 1 mL of each sample were prepared in ultrapure water where NR and Py were injected. A volume of 5 μL of a 4×10^{-5} M NR stock solution in ethanol was added, giving a constant concentration of 2×10^{-7} M in 0.5% ethanol/water for all NR fluorescence measurements. A volume of 5 μL of a 1.2×10^{-4} M Py stock solution in ethanol was added, giving a constant concentration of 6×10^{-7} M in 0.5% ethanol/water for all Py fluorescence measurements. Samples were stirred overnight before fluorescence measurements, which were performed with a Spex Fluorolog 3 spectrofluorimeter at room temperature. The slit width was set at 5 nm for excitation and 5 nm for emission. All spectra were corrected for the instrumental response of the system. The cac was calculated using both the maximum emission intensity of NR (λ_{ex} = 570 nm) and the Py fluorescence intensity ratio of the third (384−385 nm) and first vibrational bands (372−374 nm) (I_3/I_1) of the emission spectra (λ_{ex} = 339 nm) in the mannan-C_{16}/water system as a function of mannan-C_{16} concentration; in both cases, the cac was estimated as the interception of two trend lines.

Sample Preparation. Lyophilized mannan-C_{16} was dispersed in ultrapure water (1 mg/mL) with stirring for 3 days at 50 °C. The resulting milky colloidal dispersion was filtered through the membrane filter (pore size 0.45 μm). Material lost during filtration was residual, as verified using the phenol−sulfuric acid method.[24]

Cryo-Field Emission Scanning Electron Microscopy (Cryo-FESEM). The mannan-C_{16} nanogel concentrated by ultrafiltration (Amicon Ultra-4 Centrifugal Filter Units, cutoff molecular weight 1×10^5) was negatively stained with phosphotungstic acid (0.01% w/v). Samples were placed into brass rivets and plunged frozen into slush nitrogen at −200 °C and then stored in liquid nitrogen and transferred to the cryo stage (Gatan, Alto 2500, U.K.) of an electronic microscope (SEM/EDS: FESEM JEOL JSM6301F/Oxford Inca Energy 350). Each sample was fractured on the cryo stage with a knife. In the microscope, the sublimation of any unwanted surface ice was carried out in the cryo chamber for 10 min at −95 °C. At −140 °C, samples were sputter coated with gold and palladium using an accelerating voltage of 10 kV. The copper antipollutant covers and protects the sample. The samples were observed at −140 °C at 15 kV. The solvent used in the preparation of the samples (water and phosphotungstic acid) was also observed as a negative control.

Dynamic Light Scattering (DLS). The size distribution and zeta potential measurements were performed in a Malvern Zetasizer NANO ZS (Malvern Instruments Limited, U.K.). For each sample (1 mL), the size was measured periodically during 6 months of storage in a polystyrene cell at 25 °C using a He−Ne laser with a 633 nm wavelength, a detector angle of 173°, and a refractive index of 1.33. The values reported correspond to the polydispersity index (pdI) and the *z*-average diameter, that is, the mean hydrodynamic diameter, and represent the mean ± SD obtained after 10 repeated measurements.

The zeta potential and size of each sample dispersed in phosphate-buffered saline (PBS 1×, pH 7.4) and in phosphate−citrate buffer (pH 2.2−8.0) were analyzed at 37 °C in a folded capillary cell. The zeta potential values were calculated using the Smoluchowski equation. The size distribution of each sample dispersed in dilutions of NaCl (0−0.6 M) and urea (0−7 M) was evaluated at 37 °C. The values reported for the mean hydrodynamic diameter and zeta potential represent the mean ± SD obtained with three independent experiments, with three repeated measurements being performed in each one.

Results and Discussion

Synthesis of Mannan-C_{16}. Amphiphilic mannan-C_{16} was synthesized in a two-step reaction. In the first step, methacrylated

(23) van Dijk-Wolthuis, W. N. E.; Tsang, S. K. Y.; Kettenes-van den Bosch, J. J.; Hennink, W. E. *Polymer* **1997**, *38*, 6235–6242.

(24) Dubois, M.; Gilles, K. A.; Hamilton, J. K.; Rebers, P. A.; Smith, F. *Anal. Chem.* **1956**, *28*, 350–356.

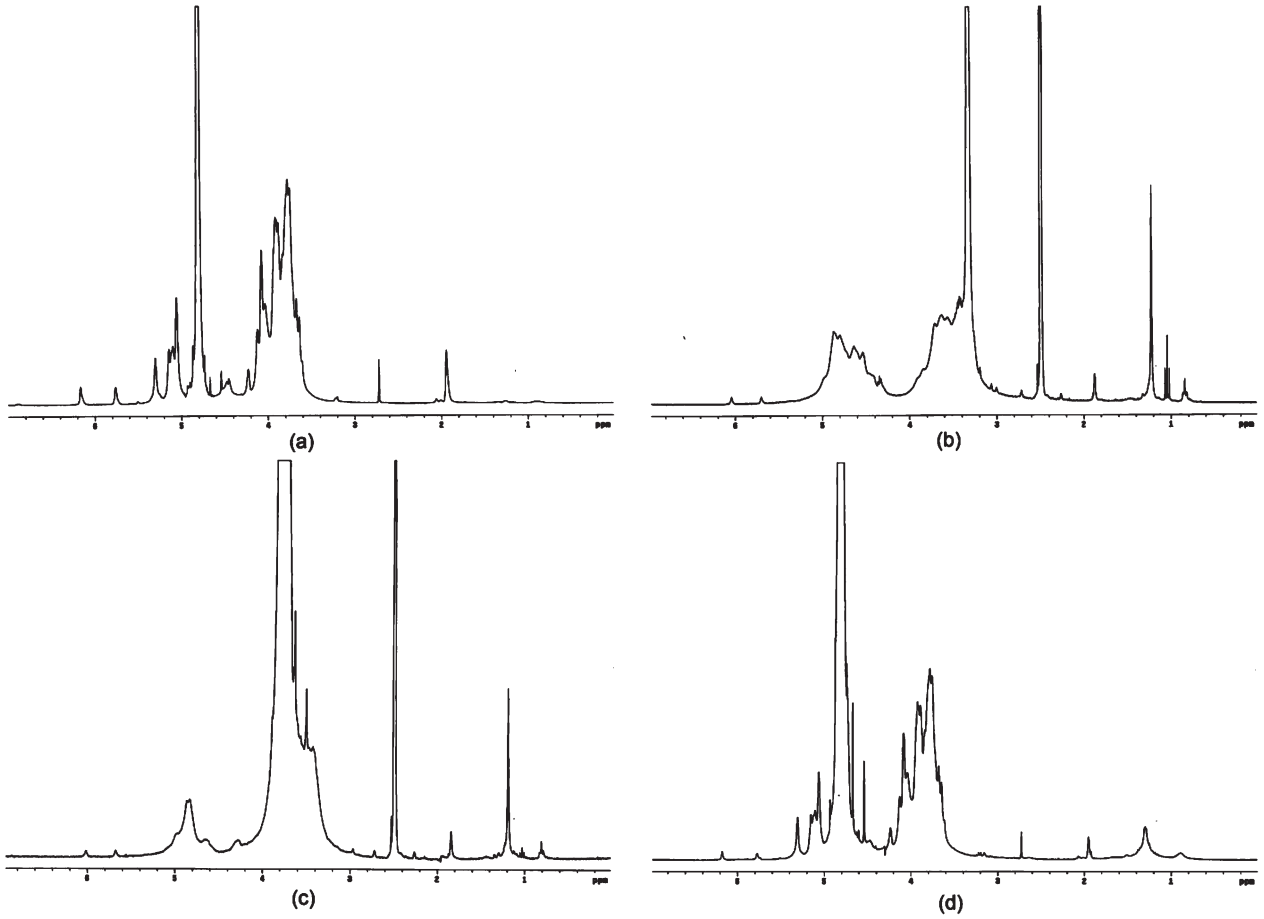

Figure 1. (a) ^{1}H NMR spectrum of mannan-HEMA (5 mg/mL) in D_2O and ^{1}H NMR spectra of mannan-C_{16} (5 mg/mL) in (b) DMSO-d_6, (c) 10% D_2O in DMSO-d_6, and (d) D_2O using MHC_{16}-6.5-1.5 as an example.

Scheme 1. Synthesis of Mannan-C_{16}

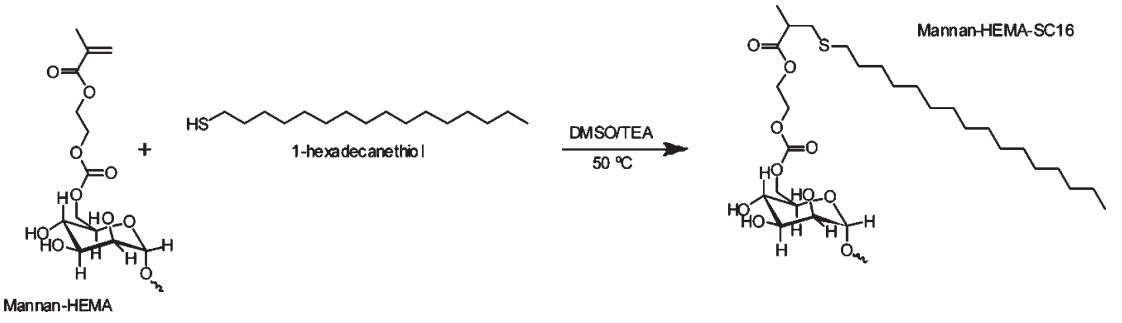

mannan was obtained by coupling HEMA-CI to mannan. A majority of HEMA groups, according to several authors, are likely coupled to the ^{6}C of the mannose residues of the grafts.[16,25] In the second step, the thiol acting as a nucleophile reacted with grafted methacrylate by a Michael addition mechanism, as shown in Scheme 1.

^{1}H NMR Measurements. The purity, chemical structure, and polymer degree of substitution (DS) of the reaction products were controlled using ^{1}H NMR spectra in D_2O, as shown in Figure 1. The characteristic peaks of the protons of the unsaturated carbons of the acrylate groups of methacrylated mannan appeared in the range of 6.18 and 5.77 ppm.[23] The successful formation of mannan-C_{16} was confirmed by the peaks appearing between 1.8 and 0.6 ppm, which correspond to the grafted alkyl moiety.[9] In both spectra, the anomeric protons of mannan can be identified because their resonances lie in the range of 4.9−5.5 ppm whereas the remaining protons of mannan appear in the range of 3.5−4.5 ppm.[26] Mannan-C_{16} was washed with *n*-hexane, and the ^{1}H NMR analysis was repeated. Because no differences were observed, it was possible to conclude that the alkyl chain was covalently bound to the methacrylate group (data not shown).

The degree of substitution of methacrylate groups (DS_{HEMA}, defined as the number of methacrylate groups per 100 mannose residues), was calculated from the ^{1}H NMR spectra of

(25) Arigita, C.; van den Berg, J.; Wensink, K.; van Steenbergen, M.; Hennink, W. E.; Crommelin, D. J. A.; Kersten, G. F. A.; Jiskoot, W. *Eur. J. Pharm. Sci.* **2004**, *21*, 131–141.

(26) Kath, F.; Kulicke, W. M. *Appl. Macromol. Chem. Phys.* **1999**, *268*, 69–80.

Table 1. Characteristics of Mannan-C_{16}

theoretical DS_{HEMA} (%)[a]	real DS_{HEMA} (%)[b]	theoretical DS_{C16} (%)[c]	real DS_{C16} (%)[d]	obtained DS_{C16} relative to methacrylated groups (%)[e]	efficiency (%)[f]	mannan-C_{16}[g]
25	5	100	0.6	12	12	MHC_{16}-5-0.6
25	5	120	1.2	24	20	MHC_{16}-5-1.2
25	5	200	4.1	82	41	MHC_{16}-5-4.1
40	6.5	120	1.5	23	19	MHC_{16}-6.5-1.5
40	6.5	200	2.5	38	19	MHC_{16}-6.5-2.5

[a] Calculated as the molar ratio of HEMA-CI to mannose residue (×100) in the reaction mixture. [b] Calculated by ^{1}H NMR of mannan-HEMA in D_2O. [c] Calculated as the molar ratio of C_{16} to HEMA (×100) in the reaction mixture. [d] Calculated by ^{1}H NMR of mannan-C_{16} in D_2O. [e] Calculated using the following equation: real $DS_{C_{16}}$/real DS_{HEMA} (×100). [f] Calculated as the ratio of the obtained to the theoretical $DS_{C_{16}}$ (×100). [g] Mannan-HEMA-SC_{16} synthesized: MHC_{16}-DS_{HEMA}-$DS_{C_{16}}$.

mannan-HEMA in D_2O with the equation $(I_a)/(I_{H1}) \times 100$, in which I_a is the average integral of the protons of the unsaturated carbons of the acrylate groups (around 6 ppm) and I_{H1} is the integral of the anomeric proton (4.9−5.5 ppm).[23] The degree of substitution with the hydrophobic alkyl chains ($DS_{C_{16}}$, defined as the number of alkyl chains per 100 mannose residues) was calculated from the ^{1}H NMR spectra of mannan-C_{16} in D_2O as $(7X)/(37Y) \times 100$, in which X is the average integral corresponding to the protons from alkyl moieties (1.8−0.6 ppm) and Y is the integral of all mannan protons (3.5−5.5 ppm).[9]

By varying the molar ratio of HEMA-CI to mannose residues and the molar ratio of C_{16} to HEMA-CI, different independent batches of mannan-C_{16} with different DS_{HEMA} and $DS_{C_{16}}$ were obtained, indicating this method to be versatile, simple, and reproducible, as shown in Table 1.

The self-assembly of amphiphilic mannan-C_{16} in water was studied using ^{1}H NMR spectroscopy. The shape and width of the proton signals of C_{16} (1.8−0.6 ppm) depend on the polarity of the solvent used to record the ^{1}H NMR spectra, as shown in Figure 1. Therefore, the association of the hydrophobic alkyl chains in forming nanogels can be detected by ^{1}H NMR. The signals provided by the methyl (0.8 ppm) and methylene (1.1 ppm) groups were sharp in DMSO-d_6 but tended to be gradually broadened at the base with an increase in the D_2O content in DMSO-d_6. A large amount of broadening was clear in pure D_2O, which is characteristic of the superposition of peaks representing a collection of chemically identical species yet possessing various degrees of mobility.[27] This result suggests that, when dispersed in water, part of the alkyl chains were exposed to hydrophobic microdomains (low mobility) but others might have been exposed to the hydrophilic solvent (high mobility). In DMSO-d_6, all hydrophobic chains were exposed to the solvent, having the same mobility, because the material is well dissolved.[9] In contrast, the mobility of the polysaccharide skeleton of mannan-C_{16} was kept in environments of different polarity. These data suggested that the mannan-C_{16} nanogel is obtained upon self-aggregation in water through the alkyl hydrophobic chains—partial water exclusion due to the hydrophobic interaction—and also owing to the relatively mobile shell of the hydrated polysaccharide skeleton on the outer surface of the nanogel.

Critical Aggregation Concentration of Mannan-C_{16}. The self-assembly of mannan-C_{16} in aqueous solutions was also studied by fluorescence spectroscopy. The cac of mannan-C_{16} with different DS values was studied using hydrophobic dyes, NR,[28] and Py,[29,30] which are poorly soluble and weakly fluorescent in water. In contrast, their solubility and fluorescence dramatically increase in a hydrophobic medium.

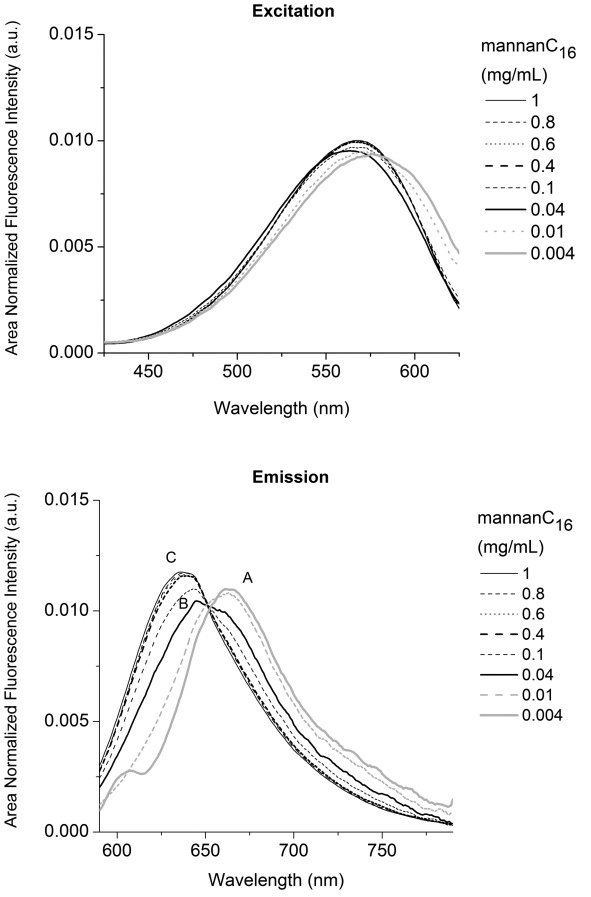

Figure 2. Area-normalized fluorescence excitation (λ_{em} = 650 nm) and emission (λ_{ex} = 570 nm) spectra of Nile red (2×10^{-7} M) in the mannan-C_{16}/water system as a function of mannan-C_{16} concentration obtained for MHC_{16}-5-0.6, as an example.

The fluorescence measurements in Figures 2 and 4 showed that for lower concentrations of mannan-C_{16}, amphiphilic molecules exist in aqueous solutions as individual molecules (premicelle aqueous environment, zone A); the fluorescence intensity of NR remained constant, without any shift in the maximum emission wavelength. For higher concentrations, above the cac, an increase in intensity associated with a strong blue shift was observed, which is attributed to NR being close to (or inside) mannan-C_{16} hydrophobic domains. These hydrophobic domains are of two types with different hydration levels (zones B and C). However, the hydrophobic domains do not correspond to a typical surfactant system.

In the case of Py fluorescence, the spectra obtained in this study were typical of Py photophysical behavior. A red shift was

(27) Hrkach, J. S.; Peracchia, M. T.; Domb, A.; Lotan, N.; Langer, R. *Biomaterials* **1997**, *18*, 27–30.
(28) Coutinho, P. J. G.; Castanheira, E. M. S.; Rei, M. C.; Oliveira, M. E. C. D. R. *J. Phys. Chem. B* **2002**, *106*, 12841–12846.
(29) Kalyanasundaram, K.; Thomas, J. K. *J. Am. Chem. Soc.* **1977**, *99*, 2039–2044.
(30) Dong, D. C.; Winnik, M. A. *Can. J. Chem.* **1984**, *62*, 2560–2565.

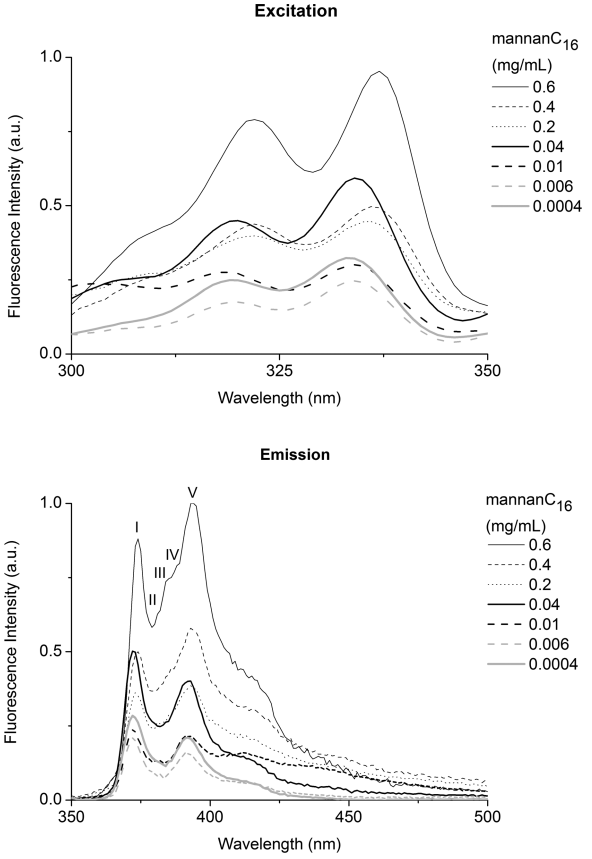

Figure 3. Fluorescence excitation (λ_{em} = 390 nm) and emission (λ_{ex} = 339 nm) spectra of pyrene (6×10^{-7} M) in the mannan-C_{16}/water system as a function of mannan-C_{16} concentration obtained for MHC_{16}-5-0.6, as an example.

observed in the excitation spectra, and the intensity increased with increasing concentration of mannan-C_{16}, as shown in Figure 3. I_3/I_1 oscillated with a linear trend below the cac value, but a small I_3/I_1 increase above this value was observed, as shown in Figure 4. This transition of intensity reflected the transference of Py to a less polar micellar domain, which was coincident with the onset of the supramolecular formation of mannan-C_{16}. However, some bands in the 450 nm region still appear above cac. This indicates the presence of Py dimers and can be explained by the high water penetration into the nanogel and is consistent with the ^{1}H NMR measurements.

The increase in the mannan-C_{16} concentration corresponds to an increased number of hydrophobic domains, allowing the solubility of more NR and Py; consequently, the fluorescence that is detected continues to increase. A second plateau is not achieved, as shown in Figure 4, either because the highest concentration of mannan-C_{16} used was not enough to enclose all of the hydrophobic dyes and saturation was not attained or because the NR or Py molecules, although enclosed in the hydrophobic domains, are sensitive to differences in the hydration level or different degrees of exposure to water and are still redistributing to hydrophobic domains with lower hydration levels as the mannan-C_{16} concentration increases above the cac. The effect is less defined in the case of Py because of the formation of Py dimers in hydrophobic domains with greater hydration levels.

The cac values obtained by fluorescence measurements with both dyes (Table 2) were consistent and exhibit a dependence on the obtained $DS_{C_{16}}$ relative to methacrylated groups, confirming

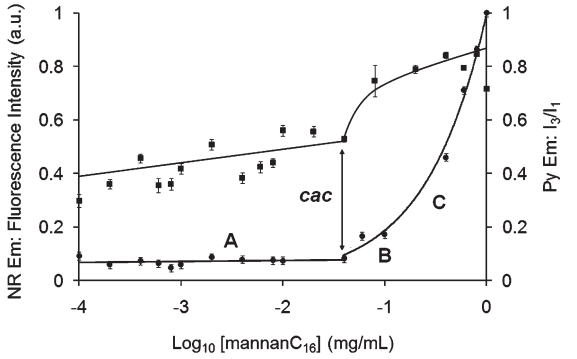

Figure 4. Maximum emission intensity of Nile red (●, λ_{ex} = 570 nm) and pyrene fluorescence intensity ratio I_3/I_1 (■, λ_{ex} = 339 nm) in the mannan-C_{16}/water system as a function of mannan-C_{16} concentration obtained for MHC_{16}-5-0.6, as an example.

Table 2. Critical Aggregation Concentration Calculated for Mannan-C_{16} by Fluorescence Spectroscopy Using Nile Red and Pyrene

	NR cac (mg/mL)	Py cac (mg/mL)
MHC_{16}-5-0.6	0.04	0.04
MHC_{16}-5-1.2	0.04	0.04
MHC_{16}-6.5-2.5	0.04	0.04
MHC_{16}-5-4.1	0.02	0.02

that C_{16} governs the propensity of these molecules to self-assemble in water. The cac was 0.04 mg/mL for lower $DS_{C_{16}}$ values relative to methacrylated group values (12% for MHC_{16}-5-0.6, 24% for MHC_{16}-5-1.2, and 38% for MHC_{16}-6.5-2.5). In contrast, for MHC_{16}-5-4.1 with $DS_{C_{16}}$ relative to acrylate groups of 82%, the cac decreased to 0.02 mg/mL.

Size and Shape of Mannan-C_{16} Nanogels. Cryo-FESEM is the most valuable technique in the visualization of the colloidal systems. Indeed, using this technique, the samples may be observed to be close to their natural state.[31] The mannan-C_{16} nanogel was heterogeneous in terms of both size and shape, as shown in Figure 5. The majority of macromolecular micelles observed may be described as imperfect spheres, with diameters ranging between 100 and 500 nm for MHC_{16}-5-1.2 and between 200 and 500 nm for MHC_{16}-6.5-2.5.

Size and Surface Charge of a Mannan-C_{16} Nanogel. The size and surface charge of a mannan-C_{16} nanogel with different DS_{HEMA} and $DS_{C_{16}}$ values were evaluated during storage and also in various environments as a function of pH and mannan-C_{16}, NaCl, and urea concentrations by studying the variation of the mean hydrodynamic diameter and zeta potential obtained using DLS. The size and surface charge of the self-assembled particulate species play important roles in determining the stability in solution, the susceptibility to aggregate disassembly, coagulation, and precipitation, and protein and cellular surface binding in vivo. Zeta potential values higher than 30 mV and lower than −30 mM are typical of colloids stabilized by electrostatic forces.

Storage. The size distribution of a mannan-C_{16} nanogel with different DS values in ultrapure water was evaluated using DLS, over a storage period of 6 months, at room temperature (25 °C). The results are shown in Figure 6. Throughout the storage period, MHC_{16}-5-1.2 kept the mean hydrodynamic diameter stable, in the range of 108−234 nm; the MHC_{16}-6.5-2.5 size oscillated in the range of 218−429 nm. Both samples exhibited fairly high polydispersity, with an average pdI of 0.63. This result was consistent with the cryo-FESEM micrographs.

Effect of the Concentration of Mannan-C_{16}. The micellar size is mainly determined by the hydrophobic forces that sequester

(31) Krauel, K.; Girvan, L.; Hook, S.; Rades, T. *Micron* **2007**, *38*, 796–803.

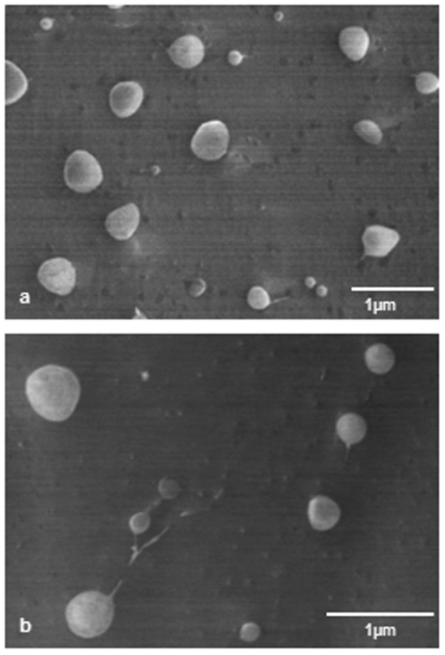

Figure 5. Cryo-FESEM negatively stained micrographs of a mannan-C_{16} nanogel: (a) MHC_{16}-5-1.2 (magnification 15 000×) and (b) MHC_{16}-6.5-2.5 (magnification 30 000×).

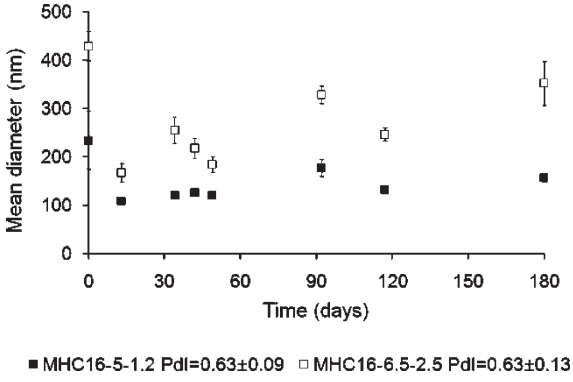

Figure 6. Size of mannan-C_{16} nanogel water dispersions (1 mg/mL) measured periodically in DLS (mean ± S.D., n = 10) over a storage period of 6 months at room temperature (25 °C).

the hydrophobic chains in the core and by the excluded volume repulsion between the chains that limits their size. The mean hydrodynamic diameter tended to be much larger for lower concentrations of mannan-C_{16}, and the material showed more instability. At 0.05 mg/mL, close to the cac, loose aggregates were formed that contained a significant quantity of solvent inside. For higher concentrations, the equilibrium favored nanogel formation. Micelles adopt their low-energy-state configuration while the remaining solvent is gradually released from the hydrophobic core, resulting in a decrease in nanogel size.[32] These results are in agreement with the two types of hydrophobic environments with different hydration levels observed with NR and Py fluorescence. Amphiphilic mannan-C_{16} resulted in mannan being randomly substituted with hydrophobic alkyl chains. In randomly modified polymers, hydrophobic and hydrophilic parts are entangled together, which permits interaction between the core and the aqueous media. Exposed hydrophobic cores within a less mobile shell formed by hydrophilic chains may result in the secondary

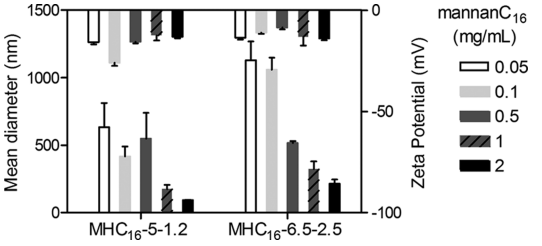

Figure 7. Influence of concentration on the size and zeta potential of mannan-C_{16} nanogel water dispersions (0.05−2 mg/mL) at 37 °C. The results shown were calculated via DLS (mean ± S.D., n = 3).

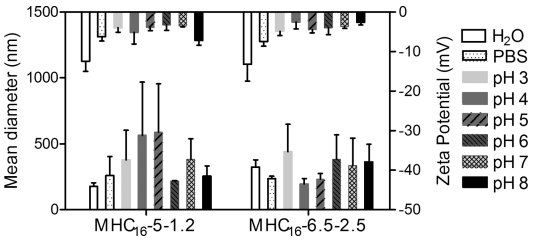

Figure 8. Influence of pH on the size and zeta potential of mannan-C_{16} nanogel dispersions (1 mg/mL) at 37 °C in water, phosphate-buffered saline (PBS 1×, pH 7.4), and phosphate−citrate buffer (pH 2.2−8.0). The results shown were calculated via DLS (mean ± S.D., n = 3).

aggregation of polymeric micelles, which might explain the presence of large macromolecular micelles for lower concentrations of mannan-C_{16}.[32]

The zeta potential of the mannan-C_{16} nanogel was apparently unaffected by the variation in concentration of mannan-C_{16} ranging between −8 and −26 mV, as shown in Figure 7. Thus, because the electrostatic forces are apparently not strong enough, the stability of the nanogel might be due to the hydration forces.

Effect of pH. The size distributions and zeta potential of mannan-C_{16} studied as a function of pH using phosphate-citrate buffer (pH 2.2−8.0) were compared to values obtained in water and PBS (Figure 8). The mean hydrodynamic diameter values obtained for MHC_{16}-5-1.2 were larger in strong acidic solutions than in neutral, basic, and PBS solutions. The smallest size was observed at pH 6, although it was slightly larger than in water. The mean hydrodynamic diameter values for MHC_{16}-6.5-2.5 were smaller in pH 4 and 5 and PBS solutions; in other pH solutions, the nanogel presented a size as obtained in water yet with higher instability. For both materials, in all solutions, zeta potential values were found to be negative but still close to zero in the region of −2 to −13 mV. This is a relative small value indicating little repulsion between macromolecular micelles to prevent aggregation. However, even with the zeta potential close to zero in some environments, the nanogel is shown to be stable on the nanoscale. The nearly neutral charge is valuable for in vivo use because large positive or negative charges may be rapidly cleared from the blood. Positively charged polymers and nanogels cause nonspecific cell sticking, and negatively charged polymers and nanogels are efficiently taken up by scavenger endothelial cells or "professional pinocytes" found in the liver.[33]

Effect of Ionic Strength. Salts are known to have the ability to destabilize colloidal systems by removing the electrostatic barrier that prevents micelle aggregation. When added in enough quantity to a stable dispersion, salts may neutralize the surface charge of the macromolecular micelles, which removes the repulsive

(32) Jones, M. C.; Leroux, J. C. *Eur. J. Pharm. Biopharm.* **1999**, *48*, 101–111.

(33) Smedsrod, B. *Comp. Hepatol.* **2004**, *3*(Suppl 1), S22.

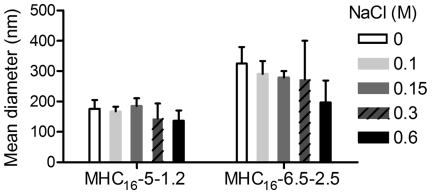

Figure 9. Influence of NaCl on the size of mannan-C_{16} nanogel dispersions (1 mg/mL) at 37 °C in NaCl solution (0−0.6 M). The results shown were calculated in DLS (mean ± S.D., $n = 3$).

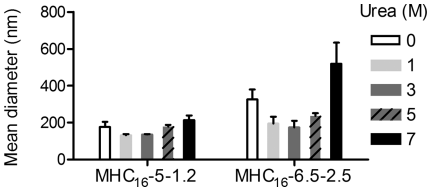

Figure 10. Influence of urea on the size of mannan-C_{16} nanogel dispersions (1 mg/mL) at 37 °C in urea solution (0−7 M). The results shown were calculated in DLS (mean ± S.D., $n = 3$).

forces that keep micelles separate and allows for coagulation due to van der Waals forces. Compared to that in salt-free solution, the mean hydrodynamic diameter for MHC_{16}-5-1.2 decreased when the NaCl concentration was 0.3 and 0.6 M. A slight instability was observed for MHC_{16}-6.5-2.5 because the mean hydrodynamic diameter decreased when the NaCl concentration was between 0.1 and 0.3 M but leveled off when a higher concentration of NaCl (0.6 M) was applied, as shown in Figure 9. No flocculation was observed. The results obtained showed that NaCl, at tested concentrations, was not able to destabilize the size of the mannan-C_{16} colloidal system.

Although the Derjaguin−Landau−Verwey−Overbeek (DLVO) theory effectively explains the long-range interaction forces observed in a large number of systems, when two surfaces or micelles are a few nanometers apart, the interactions between two solid surfaces in a liquid medium fail to be accounted for and can be much stronger. The other additional non-DLVO forces, such as the solvation force, hydrophobic force, or steric force, can be monotonically repulsive, monotonically attractive, or even oscillatory. The solvation forces referred to as hydration forces, when the solvent is water, depend both on the chemical and physical properties of the surfaces (e.g., wettability, crystal structure, surface morphology, and rigidity) and on the properties of the intervening medium.[34] The physical mechanisms underlying the hydration force might be the anomalous polarization of water near the interfaces, which completely alters its dielectric response. Instead, the repulsive forces might be due to the entropic (osmotic) repulsion of thermally excited molecular groups that protrude from the surfaces, which explains many experimental observations in neutral systems.[34] The observed stability of the nanogel (no aggregation or flocculation is observed) with increasing ionic strength thus suggests that non-DLVO forces are relevant to the colloidal behavior of this nanogel. Besides hydration forces, steric effects, which play a role whenever a reduction in the degree of freedom of the molecules in interacting colloids contributes to the stabilization of those colloids, may also be relevant in the present case.

Effect of Urea. Urea has been described as being able to break intramolecular hydrogen bonds and to destabilize hydrophobic domains.[35,36] The mean hydrodynamic diameter obtained for MHC_{16}-5-1.2 in water (176 nm) was similar to that obtained in 5 M urea, larger than that in 1 and 3 M urea, and smaller than that in 7 M urea (214 nm). A stronger variability was observed for MHC_{16}-6.5-2.5 because the mean hydrodynamic diameter was smaller than in water (325 nm) for urea at concentrations between 1 and 5 M and significantly larger for urea at 7 M (519 nm), as shown in Figure 10. Although the changeability in the experimental results, urea did not significantly affect the self-assembly of the amphiphilic system in water and consequently nanogel formation.

The nanogels have been developed as a key strategy to deliver conventional drugs, recombinant proteins, vaccines, and nucleotides, transforming their kinetics, body distribution, and bioavailability. Nanoformulations will require controllable features, such as dimension (diameter < 200 nm), nearly neutral surface charge, stability for prolonged circulation in blood, nontoxicity to cells, proper degradability (to modulate the release of encapsulated biomolecules and to enable the removal of an empty device after drug release from the body), bioconjugation to targeted cells, high-loading efficiency, and controllable release of encapsulated therapeutics, reducing undesired side effects.[37−40]

The low cac values of mannan-C_{16} indicate the thermodynamic stability of self-aggregates under dilute conditions. The cac might be further reduced by increasing the hydrophobicity, augmenting $DS_{C_{16}}$. Because polymeric micelles suffer dilution upon intravenous administration (usually about a 25-fold dilution for a bolus injection or a much higher dilution at infusion), this low cac is advantageous to maintaining the micellar structure that facilitates prolonged circulation in the bloodstream.[41,42] All polymers are characterized by a concentration window suitable for each delivery application because below the cac the micelles may be destroyed early, releasing the encapsulated therapeutic molecule before attaining its target, and because above a critical value micelle aggregation and precipitation might occur.[42,43]

Supramolecular self-assembled mannan-C_{16} might be useful in designing polymeric multifunctional nanocarriers (e.g., nanotheranostics, i.e. complementation of diagnostic tools with therapeutic modalities) because it bears functional groups for modification purposes, has adjustable chemical and mechanical properties, undergoes size alteration in a controlled manner depending on the DS of the amphiphile, and has a high water content.

Those nanogels have an interior network for the possible incorporation of hydrophobic therapeutics, physically protecting them, by hydrophilic polymer chains, from degradation in vivo. The nanoencapsulation and controllable release of therapeutics will simplify their delivery or enhance their efficacy because therapeutics become more stable, or active, and are more efficiently delivered to targeted cells.

The mannan-C_{16} nanogel has a large surface area and functional groups for potential multivalent bioconjugation. The conjugation with cell-targeting ligands recognizing specific cellular receptors, in attempting to mimic endogenous immunoglobulins, is an approach for efficient systemic active targeted delivery to specific cells of encapsulated biological agents and drugs. As a

(34) Liang, Y.; Hilal, N.; Langston, P.; Starov, V. *Adv. Colloid Interface Sci.* **2007**, *134−135*, 151–166.
(35) Mukerjee, P.; Ray, A. *J. Phys. Chem.* **1963**, *67*, 190–192.
(36) Moore, D. R.; Mathias, L. J. *J. Appl. Polym. Sci.* **1986**, *32*, 6299–6315.
(37) Hamidi, M.; Azadi, A.; Rafiei, P. *Adv. Drug Delivery Rev.* **2008**, *60*, 1638–1649.
(38) Oh, J. K.; Lee, D. I.; Park, J. M. *Prog. Polym. Sci.* **2009**, *34*, 1261–1282.
(39) Vinogradov, S. V. *Nanomedicine* **2010**, *5*, 165–168.
(40) Kabanov, A. V.; Vinogradov, S. V. *Angew. Chem., Int. Ed.* **2009**, *48*, 5418–5429.
(41) Lee, K. Y.; Jo, W. H.; Kwon, I. C.; Kim, Y.-H.; Jeong, S. Y. *Langmuir* **1998**, *14*, 2329–2332.
(42) Rapoport, N. *Prog. Polym. Sci.* **2007**, *32*, 962–990.
(43) Rijcken, C. J. F.; Soga, O.; Hennink, W. E.; van Nostrum, C. F. *J. Controlled Release* **2007**, *120*, 131–148.

polymer of mannose, mannan-C_{16} potentially targets the mannose receptor and possibly will activate professional APCs. Cell-surface-bound receptors represent suitable attractive entry sites for delivery into cells by the receptor-mediated endocytosis of specific drugs, genes, or antigens conjugated with macromolecules or supramolecular structures.[19] Mannan-C_{16} originates imperfect spheres, and spherical particles are subject to more efficient phagocytosis than ellipsoid or disk-shaped ones, being captured by macrophages.[38] Therefore, this novel nanogel has the potential to serve as a universal protein-based vaccine adjuvant and carrier capable of inducing strong immune responses.

Further work is required to continue characterizing the mannan-C_{16} nanogel and its potential as a multifunctional nanocarrier for biomedical applications.

Conclusions

The synthesis method used for amphiphilic mannan-C_{16} was showed to be versatile, simple, and reproducible. Above the cac, mannan-C_{16} formed nanosized aggregates under aqueous conditions by the association of the hydrophobic alkyl chains. The cac, determined by fluorescence spectroscopy with NR and Py, was consistent and dependent on the obtained $DS_{C_{16}}$ relative to methacrylated groups, ranging between 0.02 and 0.04 mg/mL. Cryo-FESEM revealed heterogeneous mannan-C_{16} macromolecular micelles to be similar to imperfect spheres with different diameters ranging from 100 to 500 nm. Mannan-C_{16} with higher DS_{HEMA} and $DS_{C_{16}}$ values presented larger values of the mean hydrodynamic diameter, in which oscillations denoted some instability during 6 months of storage at room temperature (25 °C). The mean hydrodynamic diameter tended to be much larger as the concentration decreased to close to the cac. For both materials, the size distribution varied on the nanoscale at different pH values. The effects of salt and urea were stronger for the highest concentrations tested and more marked for mannan-C_{16} with higher DS_{HEMA} and $DS_{C_{16}}$ but without avoiding nanogel formation and size stability. The mannan-C_{16} nanogel under tested conditions was always negatively charged with a zeta potential close to zero.

Further work is required to clarify and optimize the characteristics of these multifunctional nanogels made of mannan as a water-soluble delivery system for drugs or peptides and proteins acting, for example, like antigens or antibodies, as new strategies to target certain disease sites and thus increase the therapeutic benefit while minimizing side effects.

Acknowledgment. Financial support by International Iberian Nanotechnology Laboratory (INL) and the FCT, through the PTDC, is gratefully acknowledged.